energies

MDPI

Article

Design of Outer-Rotor Permanent-Magnet-Assisted Synchronous Reluctance Motor for Electric Vehicles

Armagan Bozkurt [1,*], Ahmet Fevzi Baba [2] and Yusuf Oner [3]

[1] Faculty of Technical Education, Pamukkale University, Denizli 20160, Turkey
[2] Faculty of Technology, Marmara University, Istanbul 34722, Turkey; fbaba@marmara.edu.tr
[3] Faculty of Engineering, Pamukkale University, Denizli 20160, Turkey; yoner@pau.edu.tr
* Correspondence: armbozkurt@pau.edu.tr

Abstract: Today's automotive industry has focused its studies on electric vehicles (EVs) or hybrid electric vehicles (HEVs) rather than gasoline-powered vehicles. For this reason, more investment has been made in electric motors with high efficiency, high torque density, and high-power factor to be used in both EVs and HEVs. In this study, an outer-rotor permanent-magnet-assisted synchronous reluctance motor (PMaSynRM) with a new rotor topology was designed for use in an EV. The design has a transversally laminated anisotropic (TLA) rotor structure. In addition, neodymium-iron-boron (NdFeB) magnets were used in rotor topology. The stator slots were designed as distributed windings, so torque ripples are minimized. At the same time, the maximum electromagnetic torque was achieved. The analysis of the designed motor was carried out using the finite element method (FEM). Optimal values of motor parameters were obtained by improving the rotor geometry of the three-phase PMaSynRM in order to obtain maximum torque and minimum torque ripple in the design. The motor is in a 48/8 slot/pole combination, a speed of 750 rpm and a power of 1 kW. The simulation results showed that the design achieved maximum torque and minimum torque ripple.

Keywords: design; FEM; outer rotor; PMaSynRM; synchronous reluctance motor (SynRM)

Citation: Bozkurt, A.; Baba, A.F.; Oner, Y. Design of Outer-Rotor Permanent-Magnet-Assisted Synchronous Reluctance Motor for Electric Vehicles. *Energies* **2021**, *14*, 3739. https://doi.org/10.3390/en14133739

Academic Editor: Felix Barreras

Received: 23 May 2021
Accepted: 18 June 2021
Published: 22 June 2021

1. Introduction

With the decrease in fossil fuels in recent years, new alternative energy sources have been sought. One of the sectors using fossil fuels is the automotive sector [1]. In the automotive sector, studies on electric vehicles (EVs) or hybrid electric vehicles (HEVs) rather than gasoline vehicles have increased in number. With the achievement of high performance in electric motors and the reduction of costs, studies on EVs in the automotive industry have risen [2]. Features required for an electric motor to be used in an EV are to obtain high torque at low speeds during start-off or when climbing a hill and at the same time to obtain high power at high speeds while cruising. In addition to these, torque ripple and acoustic noise must be minimal to achieve a good ride in an EV [3]. The motors used in EVs have been designed with either an inner rotor or outer rotor. While mechanical differentials and gear systems have been used in an internal rotor motor, the outer rotor motor is mounted directly inside the wheel [1]. Induction motors (IMs), brushless DC (BLDC) permanent magnet (PM) motors, surface mount permanent magnet motors (SPMs), interior permanent magnet motors (IPMs) and switched reluctance motors (SRMs) have been designed as in-wheel motors in both EVs and HEVs [4]. Features sought in these motors include fast torque response and power density, wide speed range, high efficiency, high reliability, and low cost [5]. PMs used in permanent magnet synchronous motors (PMSMs) are preferred due to their high energy density, but the cost of PMs has created a disadvantage [6]. IMs are suitable for use in traction vehicles due to their reliability, robustness, and low maintenance. However, their efficiency and power coefficients are small, the rate of inverter usage is low [7], and the battery duration is disadvantageous due to the high starting currents [5]. SRMs have high efficiency, low cost, simple and robust

construction, are simple to control, and can operate in a fixed power range. However, they have high noise, vibration, and torque ripple [8]. BLDC motors have high efficiency and high power density. However, since they operate in a fixed power zone, they limit the extended speed ranges [7].

In recent years, many researchers have developed SynRM and PMaSynRM rotor designs for HEVs and EVs [9]. If several flux barriers are placed per pole in the rotor topology in the SynRM design, the structure of the rotor is simple and robust. It can also work properly at low losses and high temperatures. However, SynRM has a disadvantage due to its high torque ripple and low power factor [10]. PMaSynRM is obtained by placing PMs in the flux barriers in the rotor topology to improve the low power factor and increase the low torque density as well as efficiency [11]. Due to the partial placement of PMs in the rotor flux barriers of SynRM, the cost will be lower than the cost of PM used in PMSMs.

The rotor topology of PMaSynRM is achieved by placing PMs on the rotor flux barriers of the SynRM, thus indirectly increasing the difference between the inductances of this machine [12]. Maximum performance is obtained in PMaSynRM when maximum L_d and minimum L_q are obtained in the geometric design of the rotor of PMaSynRM. That is, higher torque will be obtained with higher saliency ratio [2]. PMaSynRM generates both magnetic torque and reluctance torque. These torques depend on the flux barrier shapes in the rotor topology. Flux barrier shapes can be arc-shaped or rectangular [12].

PMaSynRM has received great attention from researchers in recent years. In the literature, a new type of hybrid-PM-powered SynRM with a smaller amount of rare earth PM to the Ferrite PM-powered SynRM has been proposed, and also the low-cost advantage of ferrite material is preserved in [6]. In [13], a 3 hp, 4-pole PMaSynRM lab prototype by placing ferrite magnets inside the rotor of a SynRM was designed and performed experimental measurements under various loading conditions. In [14], using a macroscopic design parameter based on the magnetic reluctance concept called the isolation rate along the q-axis, a simple and fast design procedure of a SynRM was introduced, and then, the performance increase of the motor was investigated by placing PMs on the rotor body. A new topology for PMaSynRM to increase the use of magnetic flux of PMs, and also to increase the full utilization of torque components (reluctance and magnetic) in PMaSynRM was presented in [15]. In [16], the optimum five-phase rare earth free external rotor ferrite-powered synchronous reluctance motor (EFaSynRM) as an alternative to internal rotor SRMs and internal PM motors for traction applications such as EVs and HEVs was proposed. A SynRM with or without PM for traction applications in electric vehicles was analyzed and the effect of rotor design on SynRM performance with experimental test results was demonstrated in [17]. In [18], a new five-phase external rotor ferrite permanent magnet-assisted synchronous reluctance motor (Fe-PMaSynRM) with a high saliency ratio was designed.

In this study, a three-phase outer rotor PMaSynRM with a power of 1 kW and a speed of 750 rpm was designed. The stator and rotor geometric structures of the designed motor were determined. The combination of slots/poles values of the motor was selected as 48 slots/8 poles. Its windings were designated as a distributed double layer winding and the rotor structure were improved to achieve maximum torque and minimum torque ripple. By performing the necessary magnetic analyzes, an efficiency of 91.30% was achieved.

2. Design Process

In this study, a three-phase outer rotor PMaSynRM was designed with a power of 1 kW to be mounted inside the wheel for use in lightweight electric vehicles. ANSYS Maxwell software was used for design and analysis. Boundary conditions and all starting characteristics of the designed PMaSynRM are given in Table 1.

Table 1. Boundary conditions and starting characteristics.

Parameter	Value
Number of phases	3
Rated power (W)	1000
Rated torque (Nm)	12.73
Rated speed (rpm)	750
Rated current (rms) (A)	<13
Slot/pole configuration	48 slots and 8 poles
Rotor outer diameter (mm)	265
Stator outer diameter (mm)	193
Stack length (mm)	80
Air-gap length (mm)	1
Steel Material	M470-50A
Magnet Material	N35H
Frequency (Hz)	50
Phase Voltage (V)	36
Efficiency	>90%

To design a three-phase outer rotor PMaSynRM motor with high torque and high-power density, we first started by creating a good slot/pole combination. The PMaSynRM stator structure is similar to the stator structure of an IM. In this study, the combination providing optimized minimum torque ripple was chosen as 48 slots/8 poles. The quarter section of the PMaSynRM is shown in Figure 1.

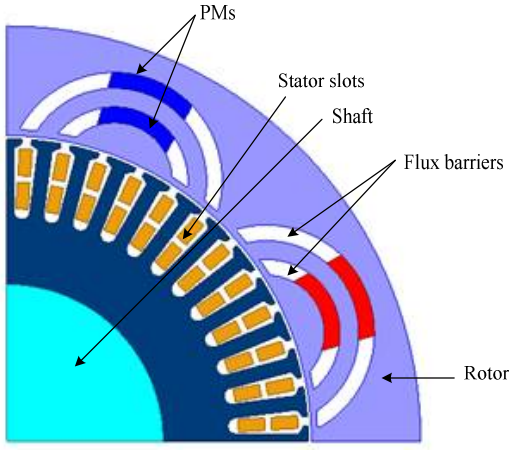

Figure 1. The quarter section of the PMaSynRM.

The stator winding can be either distributed winding or concentrated winding type. The distributed winding creates a more uniform magneto motor force (MMF) with less harmonic content [19]. It also gives a lower torque ripple compared to concentrated winding [20]. For these reasons, double-layer distributed winding was chosen as the winding type. This motor was designed for use in lightweight electric vehicles. Therefore, the disadvantages of distributed winding, such as the fact that it cannot be automated, and therefore not competitive, were been considered. Only the low torque ripple value was targeted.

The PMaSynRM with the outer rotor provides higher output torque at low speed. The electromagnetic torque generated in Equation (1) depends on the number of poles (p), the

number of phases (m), the PM flux link (λ_m), and the d-axis and q-axis components ($i_{sd}i_{sq}$) of the stator winding input currents.

$$T_e = \frac{m}{2}\frac{p}{2}\left[\lambda_m i_{sq} + \left(L_d - L_q\right) i_{sd} i_{sq}\right] \quad (1)$$

At the same time, electromagnetic torque is generated by magnets and depends on the difference between the d-axis inductance (L_d) and q-axis inductance (L_q). In the design, it was necessary to keep the inductance in the d-axis, that is, the flux value in the d-axis, at the maximum value, and keep the q-axis inductance value at a minimum. In order for the d-axis flux value to be at the maximum value, the flux barriers were kept wide, but an increase in the q-axis flux value is inevitable. It is the geometric parameters of the rotor that affect the motor performance the most and it is extremely important to determine these parameters in FEA [21].

In wheel-mounted direct drive applications, high output torque is often required to achieve acceleration, deceleration, and high-load climbing. However, torque ripples should also be considered. Therefore, output torque and torque ripples should be chosen as optimization targets [22]. To obtain a good magnetic flux distribution, in other words to provide a reduction in torque ripple, the position and number of rotor barriers are important [23]. Torque ripple percentage can be calculated as follows.

$$T_{rip}(\%) = \frac{T_{max} - T_{min}}{T_{avg}} \times 100 \quad (2)$$

where T_{max} and T_{min} are the maximum torque and the minimum torque, respectively, and T_{avg} is the average torque.

The main purpose of the PMaSynRM rotor design was to find an optimization process according to the parameters such as the geometry of flux barriers, air/iron ratio, barrier number, etc. While performing these processes, it was important to reach the rotor design that gives appropriate torque, power factor, torque ripple, and efficiency values to obtain the best performance values of the PMaSynRM. Some variables needed to be determined for PMaSynRM rotor design optimization [24].

2.1. Improvement

PMaSynRMs are nonlinear motors due to their strong magnetic saturation. Therefore, a significant effort was required to analyze these motors correctly [25]. In this process, the rotor design of the motor was improved by performing parametric analysis to obtain the desired high output torque and minimum torque ripple. Parameters of the rotor are shown in Figure 2.

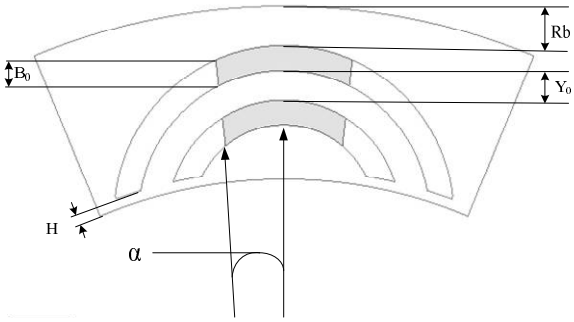

Figure 2. Rotor parameters.

During the design process, the barrier geometry was determined, and single barrier, two-barrier, three-barrier, and four-barrier rotor topologies were prepared. The designed rotor topologies are given in Figure 3.

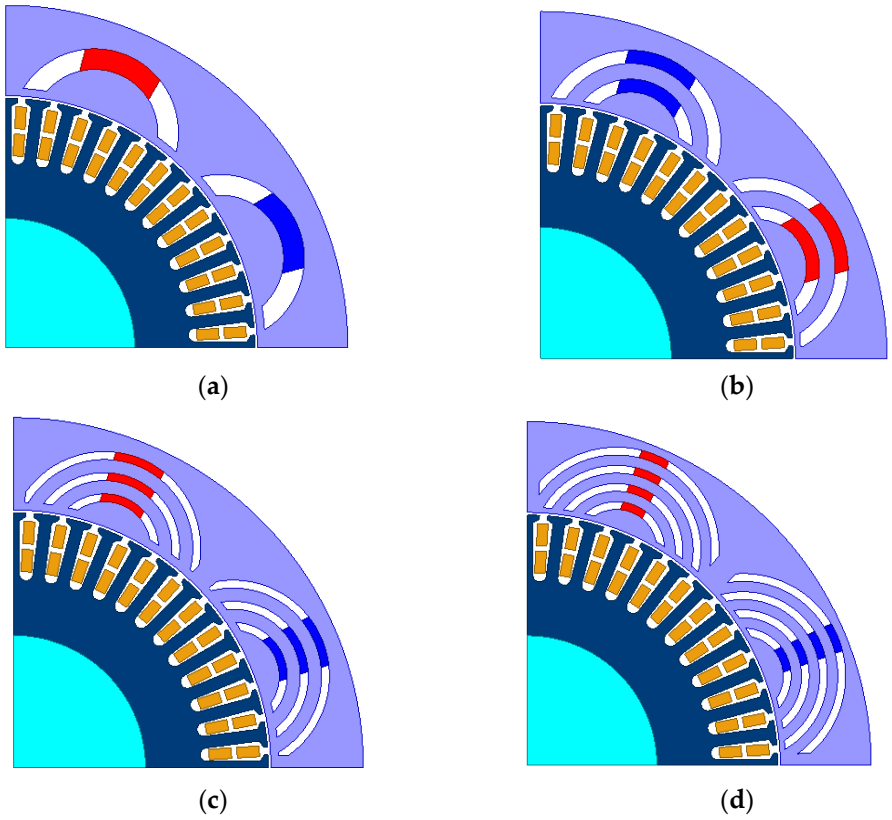

Figure 3. Designed rotor topologies (**a**) with one barrier, (**b**) with two barriers, (**c**) with three barriers and (**d**) with four barriers.

Due to its shorter completion time, current analyzes have been made on 1/8 part of each model over different values of rotor parameters. The lower and upper bounds of the rotor parameters used in parametric analyzes are given in Table 2.

Table 2. Lower and upper bounds of the rotor parameters.

Design Variables	Unit	Lower Bound	Upper Bound
α	degree	16	20
B_0	mm	3	6
Rb	mm	3	7
Y_0	mm	2.5	5
H	mm	1.5	3

Here, improvement of H, Rb, B_0, Y_0 and α values for high output torque and minimum torque ripple values after the selection of the stator and rotor parameters of the PMaSynRM is performed. The rotor design improvement algorithm is given in Figure 4. The iteration process was carried out until the desired optimal values were obtained.

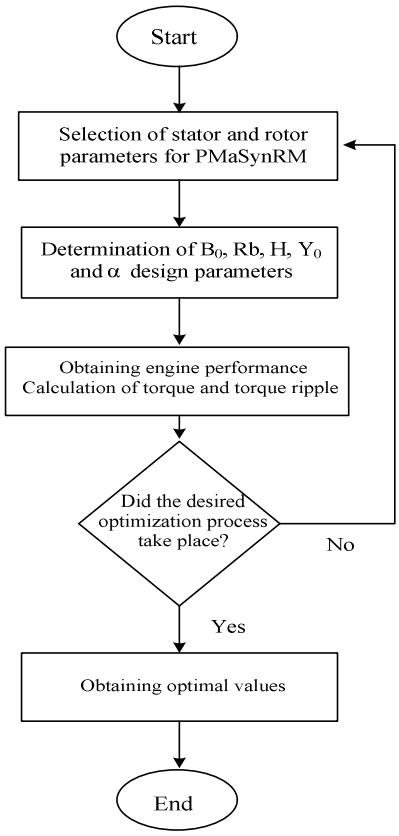

Figure 4. Improvement algorithm of rotor design.

After the parametric current analysis, the results obtained from all rotor topologies were evaluated and a three-barrier rotor topology was selected. Then, the voltage analysis was made on the whole model of the three-barrier rotor topology. Thus, appropriate torque, minimum torque ripple, and maximum efficiency values were obtained where possible at the appropriate rated current value. Within the scope of this improvement process, also the final values were obtained by changing the diameters and number of turns of the conductors used in the stator windings.

In Table 3, output torque values and torque ripple values obtained from different rotor topologies are given. As seen in Table 3, the minimum torque ripple was in the three-barrier design.

Table 3. Output torque and torque ripple values.

Number of Barriers	Output Torque (Nm)	Torque Ripple
1 barrier	12.6467	22.93%
2 barriers	12.6446	12.88%
3 barriers	12.8717	6.96%
4 barriers	12.5851	9.01%

2.2. Efficiency

The most important feature of the designed outer rotor PMaSynRM is the absence of windings in the rotor structure, and, at the same time, PMs were placed instead of the windings. In this way, the efficiency of the motor was increased. After obtaining the optimal values in the designed motor, the efficiency was also evaluated. The output power

(P_{out}) of the motor at the speed of 750 rpm was achieved as 1.010 kW, and the efficiency of the motor was obtained as 91.30% from Equation (3).

$$\eta = \frac{P_{out}}{P_{out} + P_{loss}} \quad (3)$$

where P_{out} is output power of the motor, P_{loss} is the total loss power. Total power loss is the sum of core loss, stranded loss, and other losses. Core losses are the iron losses and include eddy current losses, hysteresis losses, and additional losses. Stranded losses are ohmic losses in the windings. Other losses include friction losses and ventilation losses. The losses of the motor are given in Figure 5. Core loss was 7.4153 W, the stranded loss was 76.9017 W and other losses were 12 W.

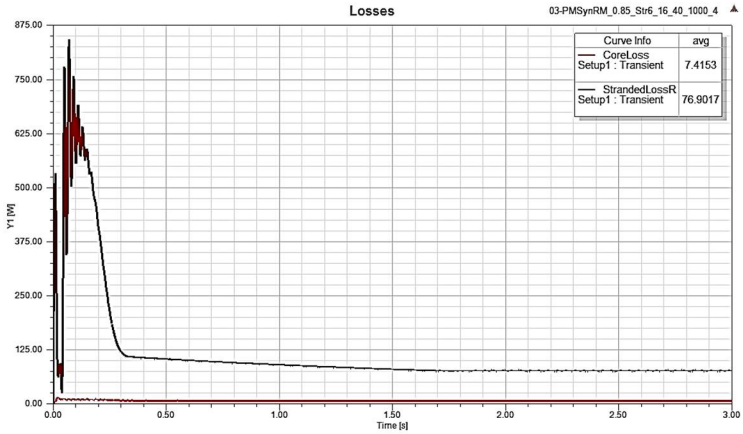

Figure 5. Losses of the designed PMaSynRM.

In traction applications, it is important to provide a wide range of constant power speeds. The main characteristics of the motor at different speeds at constant power are shown in Table 4. Torque, torque ripple, current, total loss, and efficiency values obtained in different speed ranges at constant power are given in the Table 4.

Table 4. The main characteristics of the motor at constant power at different speeds.

Speed (rpm)	500	600	750	800	1000	1200	1500
Tork (Nm)	19.09	16.10	12.87	12.21	10.05	8.07	6.47
Tork Ripple	6.09%	6.69%	6.96%	7.99%	8.25%	10.52%	12.44%
Current (A)	13.49	12.13	10.95	10.92	10.61	9.99	10.06
Total Loss (W)	137.42	115.11	96.32	94.74	90.76	81.74	82.38
Output Power (W)	999.25	1011.25	1010.87	1022.53	1052.35	1014.03	1016.15
Input Power (W)	1136.67	1126.36	1107.18	1117.27	1143.11	1095.77	1098.53
Efficiency (%)	87.91%	89.78%	91.30%	91.52%	92.06%	92.54%	92.50%

2-D and 3-D views of three phase outer rotor PMaSynRM are illustrated in Figure 6.

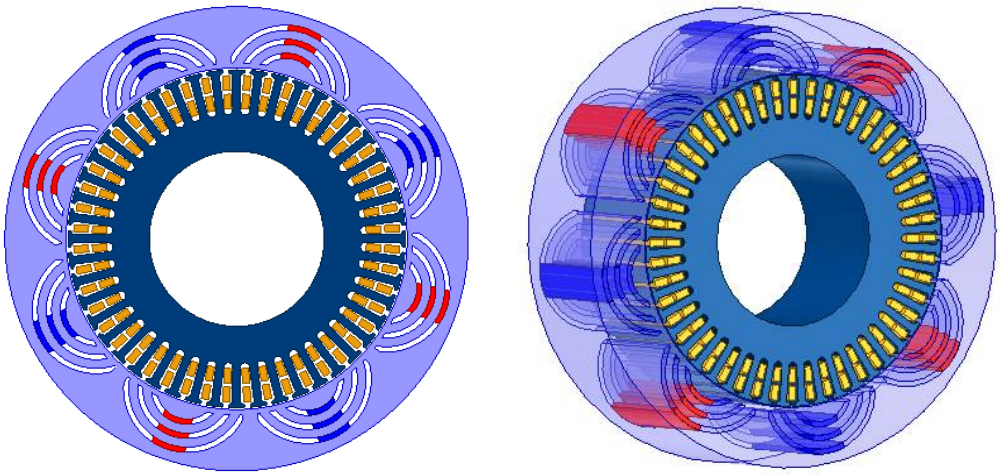

(**a**) (**b**)

Figure 6. The designed outer rotor PMaSynRM. (**a**) 2-D view and (**b**) 3-D view.

3. Simulation Results

In the simulation results of the designed PMaSynRM, the primary focus is on the output torque generation of the motor and obtaining the minimum torque ripple. This process is carried out during the optimization process. Figure 7 shows the torque behavior produced by the designed motor. The designed motor produced 12.8717 Nm of torque, and the torque ripple of the motor was 6.96%.

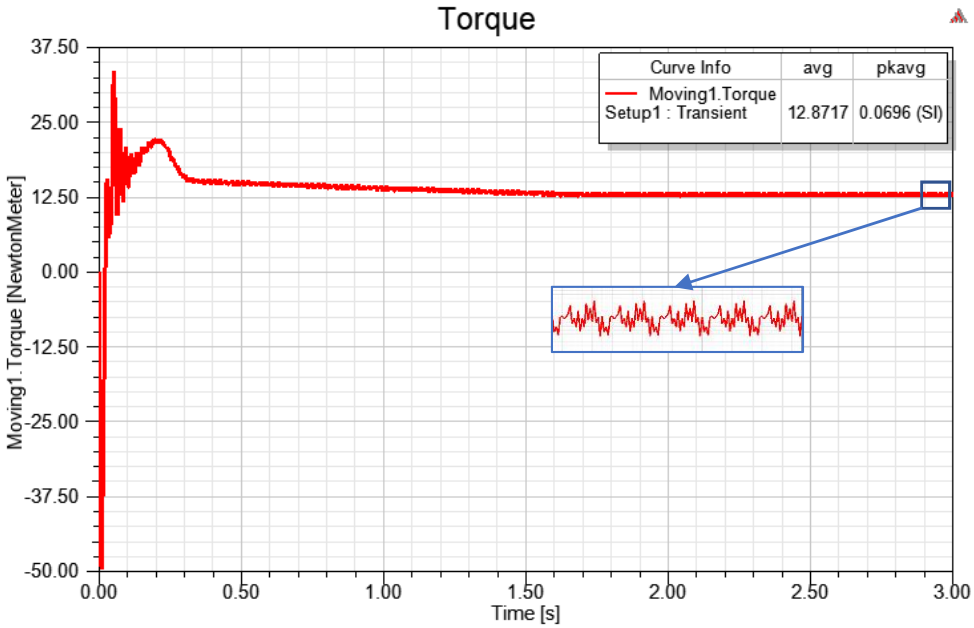

Figure 7. Torque behavior of the designed motor.

In Figure 8, speed behavior of the PMaSynRM motor is shown. It is seen that the designed motor reached the nominal speed in 0.34 s.

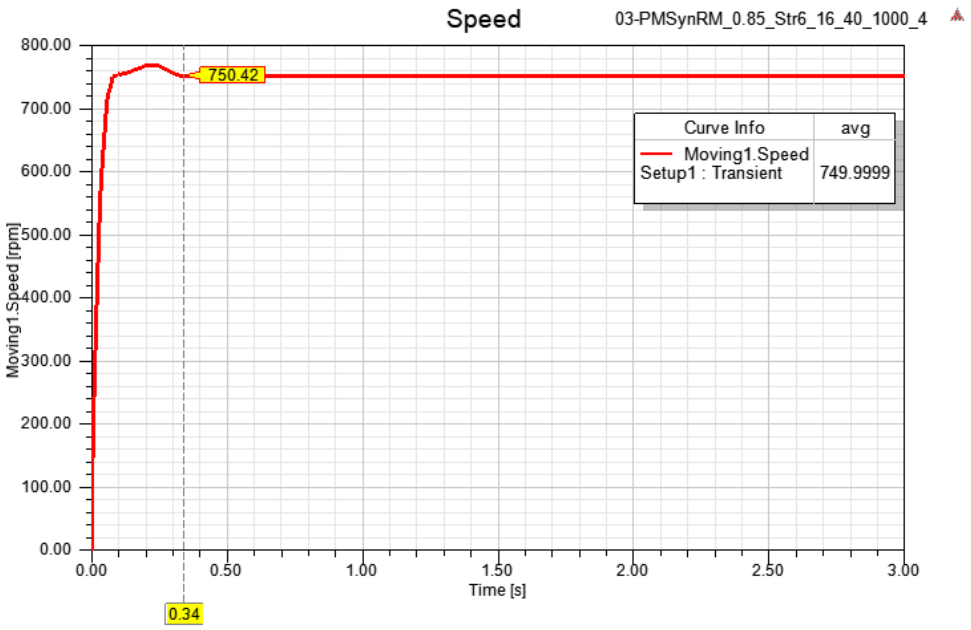

Figure 8. Speed behavior of the PMaSynRM.

In addition, the three phase currents that the designed motor draws from the stator windings is given in Figure 9. The rms value of the currents drawn from the stator windings was approximately 10.95 Amps.

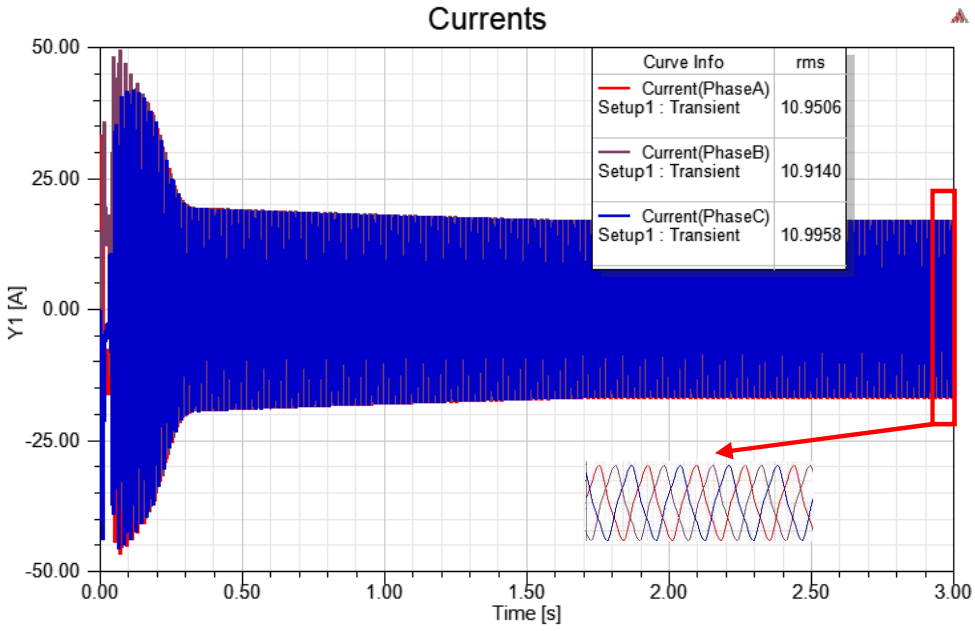

Figure 9. Three-phase currents.

The distribution of the magnetic flux lines produced by the magnets and coils of the designed motor on the stator and rotor core is shown in Figure 10.

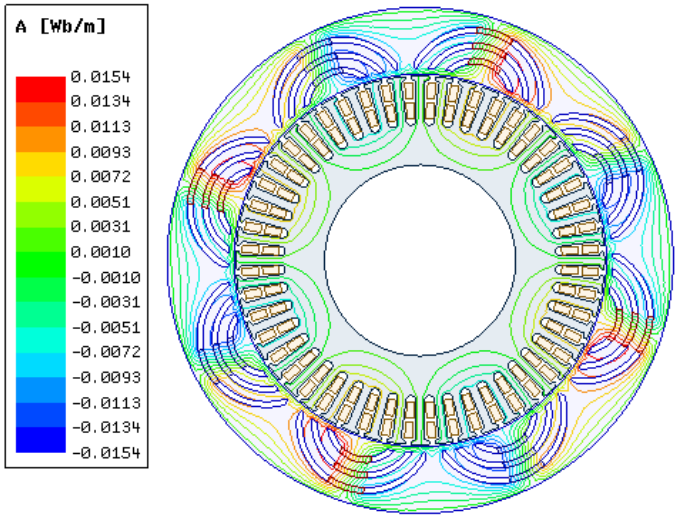

Figure 10. Flux distribution of the designed PMaSynRM.

Magnetic flux density of the PMaSynRM is shown in Figure 11. Here, it is seen that the magnetic flux density formed in the rotor and stator core was a maximum of 2 T. At the same time, a homogeneous magnetic flux distribution was realized.

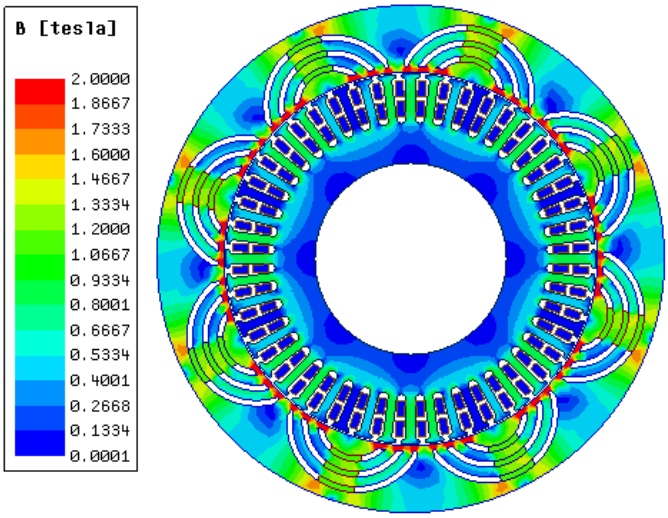

Figure 11. Magnetic flux density of PMaSynRM.

4. Conclusions

In this study, a three-phase PMaSynRM motor with the outer rotor was designed for an EV. The dimensioning of the motor was made appropriately to be placed inside the wheel of the EV to be used. After parametric analysis to obtain the desired torque value and low torque ripple, a 48 slot/8 pole combination and three-barrier rotor topology were selected. The motor was designed to operate at the speed of 750 rpm, with the power of 1 kW, and to produce 12.87 Nm of torque. At the same time, the efficiency of the designed motor was 91.30% as a result of the analysis. Since the flux densities on the stator teeth and the rotor lamination were within the desired values, the motor was operated at an operating point close to the saturation zone. In this way, a high-efficiency value was obtained. Additionally, torque ripples were minimized as far as possible with the distributed double layer winding, and the suitability of the rotor flux barriers to the combination of the number of stator slots and the number of poles were also considered in the optimization. Simulation results were obtained by 2D FEA method. As can be seen from the simulation results, the designed PMaSynRM motor provides the desired performance.

In future work, a PMaSynRM with a smaller size, different rotor topology, high power, high torque, and low torque ripple values will be designed.

Author Contributions: Conceptualization, A.B., A.F.B., Y.O.; methodology, A.B., A.F.B., Y.O.; software, A.B.; validation, A.B., A.F.B., Y.O.; investigation, A.B., A.F.B., Y.O.; performed the experiments and analyzed the data, A.B.; writing—original draft preparation, A.B.; writing—review and editing, A.B., A.F.B., Y.O.; visualization, A.B.; supervision, A.F.B., Y.O.; project administration, A.F.B., Y.O. All authors have read and agreed to the published version of the manuscript.

Funding: This research received no external funding.

Conflicts of Interest: The authors declare no conflict of interest.

References

1. Tumbek, M.; Kesler, S. Design and Implementation of a Low Power Outer-Rotor Line-Start Permanent-Magnet Synchronous Motor for Ultra-light Electric Vehicles. *Energies* **2019**, *12*, 3174. [CrossRef]
2. Moradi CheshmehBeigi, H.; Behroozi, L. Analytical Design, Electromagnetic Field Analysis and Parametric Sensitivity Analysis of An External Rotor Permanent Magnet-Assisted Synchronous Reluctance Motor. *Electr. Eng.* **2020**, *102*, 1947–1957. [CrossRef]
3. Guan, Y.; Zhu, Z.Q.; Afinowi, I.A.A.; Mipo, J.C.; Farah, P. Design of Synchronous Reluctance and Permanent Magnet Synchronous Reluctance Machines for Electric Vehicle Application. *Int. J. Comput. Math. Electr. Electron. Eng.* **2016**, *35*, 586–606. [CrossRef]
4. Bonthu, S.S.R.; Islam, M.Z.; Arafat, A.; Choi, S. Five-Phase External Rotor Permanent Magnet Assisted Synchronous Reluctance Motor for In-Wheel Applications. In Proceedings of the 2017 IEEE Transportation Electrification Conference and Expo (ITEC), Chicago, IL, USA, 22–24 June 2017; pp. 586–591.
5. Huynh, T.A.; Hsieh, M.-F. Performance Analysis of Permanent Magnet Motors for Electric Vehicles (EV) Traction Considering Driving Cycles. *Energies* **2018**, *11*, 1385. [CrossRef]
6. Wu, W.; Zhu, X.; Quan, L.; Du, Y.; Xiang, Z.; Zhu, X. Design and Analysis of a Hybrid Permanent Magnet Assisted Synchronous Reluctance Motor Considering Magnetic Saliency and PM Usage. *IEEE Trans. Appl. Supercond.* **2018**, *28*, 1–6. [CrossRef]
7. Zeraouila, M.; Benbouzid, M.E.H.; Diallo, D. Electric Motor Drive Selection Issues for HEV Propulsion Systems: A Comparative Study. In Proceedings of the IEEE Vehicle Power and Propulsion Conference, Chicago, IL, USA, 7–9 September 2005; pp. 280–287.
8. Anekunu, A.Y.; Chowdhury, S.P.; Chowdhury, S. A Review of Research and Development on Switched Reluctance Motor for Electric Vehicles. In Proceedings of the IEEE Power & Energy Society General Meeting, Vancouver, BC, Canada, 21–25 July 2013; pp. 1–5.
9. Goncalves, A.P.; Cruz, S.M.A.; Ferreira, F.J.T.E.; Mendes, A.M.S.; De Almeida, A.T. Synchronous Reluctance Motor Drive for Electric Vehicles Including Cross-Magnetic Saturation. In Proceedings of the IEEE Vehicle Power and Propulsion Conference (VPPC), Coimbra, Portugal, 27–30 October 2014; pp. 1–6.
10. Ibrahim, M.N.F.; Rashad, E.; Sergeant, P. Performance Comparison of Conventional Synchronous Reluctance Machines and PM-Assisted Types with Combined Star-Delta Winding. *Energies* **2017**, *10*, 1500. [CrossRef]
11. Morimoto, S.; Ooi, S.; Inoue, Y.; Sanada, M. Experimental Evaluation of a Rare-Earth-Free PMASynRM with Ferrite Magnets for Automotive Applications. *IEEE Trans. Ind. Electron.* **2014**, *61*, 5749–5756. [CrossRef]
12. Ashkezari, J.D.; Khajeroshanaee, H.; Niasati, M.; Mojibian, M.J. Optimum Design and Operation Analysis of Permanent Magnet-Assisted Synchronous Reluctance Motor. *Turk. J. Electr. Eng. Comput. Sci.* **2017**, *25*, 1894–1907. [CrossRef]
13. Liu, C.-T.; Luo, T.-Y.; Shih, P.-C.; Yen, S.-C.; Lin, H.-N.; Hsu, Y.-W.; Hwang, C.-C. On the Design and Construction Assessments of a Permanent-Magnet-Assisted Synchronous Reluctance Motor. *IEEE Trans. Magn.* **2017**, *53*, 1–4.
14. Aghazadeh, H.; Afjei, E.; Siadatan, A. Comprehensive Design Procedure and Manufacturing of Permanent Magnet Assisted Synchronous Reluctance Motor. *Int. J. Eng.* **2019**, *32*, 1299–1305.
15. Mohammadi, A.; Mirimani, S.M. Design and Analysis of a Novel Permanent Magnet Assisted Synchronous Reluctance Machine Using Finite-Element-Method. In Proceedings of the 11th Power Electronics, Drive Systems, and Technologies Conference (PEDSTC), Tehran, Iran, 4–6 February 2020; pp. 1–5.
16. Bonthu, S.S.R.; Islam, M.Z.; Choi, S. Design of A Rare Earth Free External Rotor Permanent Magnet Assisted Synchornous Reluctance Motor. In Proceedings of the IEEE International Electric Machines and Drives Conference (IEMDC), Miami, FL, USA, 21–24 May 2017; pp. 1–6.
17. Bianchi, N.; Bolognani, S.; Carraro, E.; Castiello, M.; Fornasiero, E. Electric Vehicle Traction Based on Synchronous Reluctance Motors. *IEEE Trans. Ind. Appl.* **2016**, *52*, 4762–4769. [CrossRef]
18. Islam, M.Z.; Choi, S.; Elbuluk, M.E.; Bonthu, S.S.R.; Arafat, A.; Baek, J. Design of External Rotor Ferrite-Assisted Synchronous Reluctance Motor for High Power Density. *Appl. Sci.* **2021**, *11*, 3102. [CrossRef]
19. Bonthu, S.S.R.; Choi, S.; Gorgani, A.; Jang, K. Design of Permanent Magnet Assisted Synchronous Reluctance Motor with External Rotor Architecture. In Proceedings of the IEEE International Electric Machines & Drives Conference (IEMDC), Coeur d'Alene, ID, USA, 10–13 May 2015; pp. 220–226.
20. EL-Refaie, A.M. Fractional-Slot Concentrated-Windings Synchronous Permanent Magnet Machines: Opportunities and Challenges. *IEEE Trans. Ind. Electron.* **2010**, *57*, 107–121. [CrossRef]

21. Aghazadeh, H.; Afjei, S.E.; Siadatan, A. Sensitivity Analysis of External-Rotor Permanent Magnet Assisted Synchronous Reluctance Motor. *World Acad. Sci. Eng. Technol. Int. J. Energy Power Eng.* **2018**, *12*, 426–430.
22. Zhu, X.; Shu, Z.; Quan, L.; Xiang, Z.; Pan, X. Multi-objective Optimization of an Outer-Rotor V-Shaped Permanent Magnet Flux Switching Motor Based on Multi-Level Design Method. *IEEE Trans. Magn.* **2016**, *52*, 1–8. [CrossRef]
23. Nagarajan, V.S.; Kamaraj, V.; Sivaramakrishnan, S. Geometrical Sensitivity Analysis Based on Design Optimization and Multi-physics Analysis of PM Assisted Synchronous Reluctance Motor. *Bull. Pol. Acad. Sci. Tech. Sci.* **2019**, *67*. [CrossRef]
24. Ersöz, M.; Öner, Y.; Bingöl, O. Akı Bariyerli TLA Tipi Senkron Motor Tasarımı ve Optimizasyonu. *J. Fac. Eng. Archit. Gazi Univ.* **2016**, *31*, 941–950.
25. Wang, Y.; Ionel, D.M.; Rallabandi, V.; Jiang, M.; Stretz, S.J. Large-Scale Optimization of Synchronous Reluctance Machines Using CE-FEA and Differential Evolution. *IEEE Trans. Ind. Appl.* **2016**, *52*, 4699–4709. [CrossRef]